Aalborg Universitet

Uplink Multiplexing of eMBB/URLLC Services Assisted by Reconfigurable Intelligent Surfaces

Souza, João Henrique Inacio de; Croisfelt, Victor; Kotaba, Radosław; Abrão, Taufik; Popovski, Petar

Publication date:
2023

Link to publication from Aalborg University

Uplink Multiplexing of eMBB/URLLC Services Assisted by Reconfigurable Intelligent Surfaces

João Henrique Inacio de Souza*, Victor Croisfelt†, Radosław Kotaba†, Taufik Abrão*, and Petar Popovski†

*Department of Electrical Engineering, Universidade Estadual de Londrina, Londrina, Brazil
†Department of Electronic Systems, Aalborg University, Aalborg, Denmark
E-mail: joaohis@outlook.com, {vcr, rak, petarp}@es.aau.dk, and taufik@uel.br

Abstract—Reconfigurable intelligent surfaces (RISs) with their potential of enabling a programmable environment comprise a promising technology to support the coexistence of enhanced mobile broadband (eMBB) and ultra-reliable-low-latency communication (URLLC) services. In this paper, we propose a RIS-assisted scheme for multiplexing hybrid eMBB-URLLC uplink traffic. Specifically, the scheme relies on the computation of two RIS configurations, given that only eMBB channel state information (CSI) is available. The first configuration optimizes the eMBB quality of service, while the second one mitigates the eMBB interference in the URLLC traffic. Analyzing the outage probability achieved by the scheme, we demonstrate that a RIS can improve the reliability of URLLC transmissions even in the absence of URLLC CSI.

Index Terms—Reconfigurable intelligent surface (RIS), enhanced mobile broadband (eMBB), ultra-reliable low-latency communications (URLLC), and interference nulling.

I. INTRODUCTION

The fifth generation (5G) of wireless communication technology and beyond are envisioned to simultaneously support heterogeneous services with different quality of service (QoS) requirements and traffic characteristics [1], [2]. In particular, enhanced mobile broadband (eMBB) require extremely high data rates, while ultra-reliable-low-latency communication (URLLC) services demand high reliability and low latency. The contrast between the requirements of these two services makes it very challenging to jointly serve eMBB and URLLC users' equipment (UEs). In the uplink (UL), this is even more difficult since UEs cannot communicate directly and, consequently, coordinate the access among themselves. This necessitates the study of UL multiplexing strategies to allow better coexistence of eMBB and URLLC UEs.

Reconfigurable intelligent surfaces (RISs) comprise an emerging technology for future wireless communication networks that can provide interesting solutions for the aforementioned problem [3]. A RIS is a thin sheet of composite material that can cover, *e.g.*, parts of walls and buildings. A RIS can reflect incident signals to desired directions by controlling/programming the configuration of the phase shifts of the many elements that compose it [4]. Besides, a *hybrid* RIS is a RIS equipped with active elements, enabling it to also digitally process the signal impinging upon it. In this work, we are interested in further studying RIS-assisted multiplexing for eMBB and URLLC services in the UL direction. In our context, there are two main deployment challenges when

designing such a RIS-assisted multiplexing strategy [3]. First, the base station (BS) is often unaware of the channel state information (CSI) and the time of arrival of a URLLC UE [1]. Second, the control and programmability of the RIS add an extra latency layer that can impact the URLLC requirements.

There is a wide literature on RIS-assisted eMBB and URLLC systems. In [3], the authors give an overview of the main challenges and potentials of enabling the coexistence of eMBB and URLLC UEs by leveraging the environment programmability of the RIS. Works such as [5], [6] consider the RIS-assisted resource allocation problem of URLLC UEs, while [7] and [8] study the achievable rates of RIS-assisted networks with short packets. RIS-assisted scheduling at the BS is studied in [9]–[12] for the downlink (DL) direction. In particular, the authors of [12] propose a two-time scale RIS-assisted scheduling and resource allocation scheme for eMBB and URLLC UEs. To attain the different QoS requirements, their scheme optimizes the precoder of a multi-antenna BS in each mini-slot while the RIS is reconfigured in each time slot to avoid extra latency due to the RIS control. Closer to our work, the authors of [13] studied the UL direction, assuming that only eMBB CSI is available at the BS to optimize the RIS phase shifts' configuration. Moreover, [14] deals with the problem of RIS-assisted grant-free random access of URLLC UEs in the UL. However, none of these works addresses the coexistence of eMBB and URLLC UEs, where the RIS supports the multiplexing of UEs, without being considered part of the scheduling scheme employed by the BS.

In this paper, we propose an UL RIS-assisted multiplexing scheme to support the coexistence of eMBB and URLLC traffic. The scheme is based on computing two RIS configurations. The first optimizes the QoS of the eMBB UE. While the second focuses on supporting the QoS of the URLLC UE based on the idea of interference nulling (IN), where reliable URLLC transmissions are made possible even in the presence of eMBB interference. The problem of IN using RIS is addressed in the recent literature [15]–[17], but it has not been applied before to support different service modes. To satisfy the URLLC low-latency requirement, our scheme relies on detecting the start of the URLLC traffic locally at a *hybrid* RIS, introducing minimum overhead and low computational complexity. Performance is analyzed by evaluating the spectral efficiency (SE) of the eMBB UE and the outage probability and latency for the URLLC one.

II. System Model

We consider the UL channel of a wideband wireless system with one single-antenna BS, one hybrid RIS, and two single-antenna UEs. The first UE uses eMBB, while the second URLLC.[1] Henceforth, we index the UEs by $\iota \in \{e, u\}$, where e and u refer to the eMBB and URLLC UE, respectively. We assume an industrial scenario where the channel links directly connecting the UEs and the BS are blocked by obstacles. Thus, the RIS is deployed to simultaneously have line-of-sight with the UEs and the BS, providing strong reflected channel links for communication. The RIS comprises $N \in \mathbb{Z}_+$ passive reflecting elements and one active receive element, placed at the center of the RIS. The RIS can perform light computational tasks by processing the signal received from its active element. The passive reflecting elements are placed into the vertices of a square grid of side $d = \lambda/2$, where $\lambda > 0$ is the carrier wavelength. Each element induces a phase shift $\theta_n \in [0, 2\pi)$ to an impinging signal with marginal impact on its amplitude. The RIS configuration is defined by the reflection matrix $\mathbf{\Psi} = \mathrm{diag}([\psi_1 \; \cdots \; \psi_N]^\mathsf{T})$, where $\psi_n = e^{-j\theta_n}$, $\{\psi_n\}_{n=1}^N$ are the reflection coefficients of the RIS elements. The BS controls the RIS via an out-of-band control channel.

A. Structure of the Uplink Frame

Fig. 1 depicts the UL frame, in which the time-frequency resources used for payload transmission are organized into a grid. In the time domain, the length of the UL frame is $T > 0$, and it is divided into $M \in \mathbb{Z}_+$ identical mini-slots of duration $T_\mathrm{m} > 0$. In the frequency domain, the spectrum dedicated to the system has the bandwidth $B > 0$, and it is divided into $R \in \mathbb{Z}_+$ identical resources of bandwidth $B_\mathrm{r} > 0$. We further assume the block-fading model, *i.e.*, the channel gains remain constant for the entire frame duration. Moreover, we consider that the eMBB UE is admitted and scheduled by the BS at the beginning of the frame, while the URLLC UE can start its transmission during any of the mini-slots of the UL frame.

Due to different requirements, the two UEs use the available time-frequency resources differently. To ensure high SE, the eMBB transmission spans over the entire frame, while using only a single frequency resource B_r. Conversely, the URLLC transmission spans over a limited number of $M_\mathrm{u} \in \mathbb{Z}_+$, $1 \leq M_\mathrm{u} \leq M$ contiguous mini-slots but over all the frequency resources so as to guarantee, respectively, the low-latency and high-reliability requirements.

B. Channel Model

Let $\mathbf{q}_\mathrm{BS}, \mathbf{q}_\mathrm{RIS}, \mathbf{q}_\mathrm{u}, \mathbf{q}_\mathrm{e} \in \mathbb{R}^3$ denote, respectively, the position vectors of the BS antenna, the center of the RIS, and the UEs. Let $\mathbf{k}(\mathbf{q}) \in \mathbb{R}^3$ denote the RIS wave vector w.r.t. a generic position $\mathbf{q} \in \mathbb{R}^3$, which is defined as

$$\mathbf{k}(\mathbf{q}) \triangleq \frac{2\pi}{\lambda} \frac{\mathbf{q} - \mathbf{q}_\mathrm{RIS}}{\|\mathbf{q} - \mathbf{q}_\mathrm{RIS}\|_2}. \tag{1}$$

[1]To attain efficient multi-user communication, the signals of multiple UEs of each traffic type must be multiplexed in the UL. However, to simplify the analysis, we considered a single UE of each traffic type, leaving the general case for a future extension of this work.
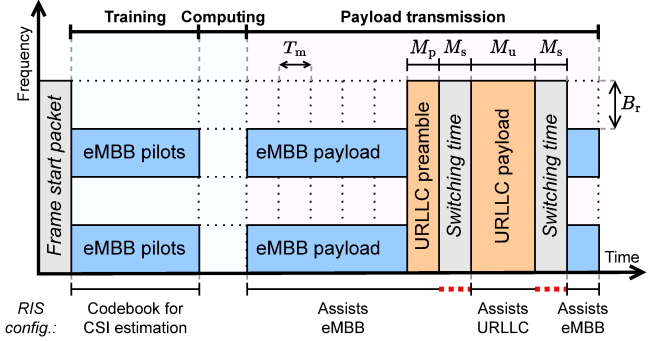

Fig. 1. Structure of the UL frame divided into training, computing, and payload transmission phases.

The RIS array response vector w.r.t. point $\mathbf{q}$, denoted by $\mathbf{a}(\mathbf{q}) \in \mathbb{C}^N$, can then be obtained as

$$\mathbf{a}(\mathbf{q}) \triangleq [e^{j\mathbf{k}(\mathbf{q})^\mathsf{T}(\mathbf{q}_{\mathrm{RIS},1} - \mathbf{q}_\mathrm{RIS})} \; \cdots \; e^{j\mathbf{k}(\mathbf{q})^\mathsf{T}(\mathbf{q}_{\mathrm{RIS},N} - \mathbf{q}_\mathrm{RIS})}]^\mathsf{T}, \tag{2}$$

where $\mathbf{q}_{\mathrm{RIS},n} \in \mathbb{R}^3$, $\forall n \in \{1, \ldots, N\}$ is the position of the n-th RIS element. Moreover, the path loss between two positions $\mathbf{q}$ and $\mathbf{q}' \in \mathbb{R}^3$ is

$$\gamma(\mathbf{q}, \mathbf{q}') \triangleq \gamma_0 \left(\frac{d_0}{\|\mathbf{q}' - \mathbf{q}\|_2} \right)^\beta, \tag{3}$$

where $\gamma_0 > 0$ is the path loss measured at the reference distance $d_0 > 0$ from the source, and $\beta > 0$ is the path loss exponent. Therefore, the channel vector $\mathbf{g} \in \mathbb{C}^{1 \times N}$ between the RIS elements and the BS antenna is

$$\mathbf{g} \triangleq \sqrt{\gamma(\mathbf{q}_\mathrm{BS}, \mathbf{q}_\mathrm{RIS})} \mathbf{a}^\mathsf{H}(\mathbf{q}_\mathrm{BS}). \tag{4}$$

Similarly, the channel vectors $\mathbf{h}_\iota \in \mathbb{C}^N$ between the RIS elements and the UEs are

$$\mathbf{h}_\iota \triangleq \sqrt{\gamma(\mathbf{q}_\iota, \mathbf{q}_\mathrm{RIS})} \mathbf{a}(\mathbf{q}_\iota). \tag{5}$$

Finally, we let $g_n = [\mathbf{g}]_n$ and $h_{\iota,n} = [\mathbf{h}_\iota]_n$ denote the channel coefficients between the n-th RIS element and the BS antenna, and the n-th RIS element and the UEs, respectively.

C. Signal Model

We index mini-slots by $m \in \{1, \ldots, M\}$. Let $\mathcal{M}_\mathrm{u} \subseteq \{1, \ldots, M\}$ with $|\mathcal{M}_\mathrm{u}| = M_\mathrm{u}$ denote the set of mini-slots where the URLLC UE transmits. We denote as $\mathbf{x}_{\iota,m} \in \mathbb{C}^L$ the vectors with the $L \in \mathbb{Z}_+$ symbols transmitted by each UE such that $\mathbb{E}\{\|\mathbf{x}_{\iota,m}\|_2^2\} = 1$. Thus, $\mathbf{x}_{\mathrm{u},m} = \mathbf{0}_L$ in the mini-slots with absence of URLLC traffic, that is, when $m \notin \mathcal{M}_\mathrm{u}$. Now, let $p_\iota > 0$ denote the UEs' transmit powers for one mini-slot. Considering the RIS configuration $\mathbf{\Psi}$, the received signal $\mathbf{y}_m(\mathbf{\Psi}) \in \mathbb{C}^L$ at the BS for a single time-frequency resource can be written as:

$$\mathbf{y}_m(\mathbf{\Psi}) \triangleq \sqrt{p_\mathrm{u}} (\mathbf{g}\mathbf{\Psi}\mathbf{h}_\mathrm{u}) \mathbf{x}_{\mathrm{u},m} + \sqrt{p_\mathrm{e}} (\mathbf{g}\mathbf{\Psi}\mathbf{h}_\mathrm{e}) \mathbf{x}_{\mathrm{e},m} + \mathbf{w}_m, \tag{6}$$

where $\mathbf{w}_m \sim \mathcal{CN}(\mathbf{0}_L, \sigma^2 \mathbf{I}_L)$ is the additive white Gaussian noise (AWGN). Using (6), the signal-to-noise ratio (SNR) for eMBB in the mini-slots without URLLC interference is:

$$\Gamma_{\mathrm{e},m}(\mathbf{\Psi}) \triangleq \frac{p_\mathrm{e} |\mathbf{g}\mathbf{\Psi}\mathbf{h}_\mathrm{e}|^2}{\sigma^2}, \; \forall m \in \{1, \ldots, M\} \backslash \mathcal{M}_\mathrm{u}. \tag{7}$$

When the URLLC signal is present, its signal-to-interference-plus-noise ratio (SINR) is given by

$$\Gamma_{\mathrm{u},m}(\boldsymbol{\Psi}) \triangleq \frac{p_{\mathrm{u}}|\mathbf{g}\boldsymbol{\Psi}\mathbf{h}_{\mathrm{u}}|^2}{p_{\mathrm{e}}|\mathbf{g}\boldsymbol{\Psi}\mathbf{h}_{\mathrm{e}}|^2 + \sigma^2}, \ \forall m \in \mathcal{M}_{\mathrm{u}}. \qquad (8)$$

With (7) and (8), one can measure the quality of the radio links established for the UEs by the RIS.

III. RIS-ASSISTED MULTIPLEXING SCHEME

Here we introduce the proposed multiplexing scheme for eMBB and URLLC traffic. As depicted in Fig. 1, the multiplexing scheme contains three phases: *training*, *computing*, and *payload transmission*. We start by detailing how each phase can be designed to satisfy the communication constraints of both traffic types. In particular, we aim to answer the question: *Relying only on eMBB CSI, how to optimize two RIS configurations to assist each UE transmission independently?* We answer this by designing two different RIS configurations, an eMBB-oriented one and another for URLLC.

A. Phases of the Multiplexing Scheme

From Fig. 1, the UL frame can be divided into the following phases. **1. Training:** During this phase, the scheduled eMBB UE transmits UL pilot symbols for CSI acquisition at the BS, while the RIS switches among configurations from a predefined configuration codebook to enable the BS to estimate the eMBB CSI [4]. **2. Computing:** The BS then estimates the cascaded eMBB UE-RIS-BS channels. This allows the BS to compute two RIS configurations: the *eMBB-oriented configuration* to assist the scheduled eMBB transmission and the *URLLC-oriented configuration* to assist a potential URLLC transmission. Finally, these two configurations are sent to the RIS to be stored there and to be used in the next phase. **3. Payload Transmission:** In this phase, the scheduled eMBB UE transmits its payload whereas the RIS starts by being configured with the eMBB-oriented configuration. If the URLLC UE has a packet to send within the mini-slots that comprise this phase, it will immediately transmit a preamble over $M_{\mathrm{p}} \in \mathbb{Z}_+$ mini-slots to announce its intention to transmit payload data. By exploiting the URLLC preamble and its active element,[2] the RIS can detect the start of the URLLC traffic. The RIS then switches to the URLLC-oriented configuration to focus on supporting the URLLC QoS. However, we consider that the time that the RIS takes to switch its configuration is in the same order as the time of a mini-slot, which is around some microseconds [1], [4], [12]. Hence, we consider the RIS takes $M_{\mathrm{s}} \in \mathbb{Z}_+$ mini-slots to switch between configurations. We also assume that the URLLC UE is aware of this *switching time* and waits for it before transmitting the payload. After the URLLC payload transmission is done, the RIS switches back to the eMBB-oriented configuration, imposing again the switching time of M_{s} mini-slots. While all this occurs, the eMBB UE continues transmitting its payload data but with a varying transmission rate due to the changes in the environment caused

by the RIS. Moreover, the BS handles the scheduling of the UEs and its services, while being totally transparent to the RIS operation, that is, the BS does not communicate/control the RIS until the start of the next UL frame.

Our proposal of carrying out the URLLC preamble detection locally at the RIS could be an essential building block to enable low-latency URLLC transmissions, since it avoids extra overhead of communicating with the BS while still improving the channel conditions of the URLLC UE. However, the successful decoding of the URLLC payload data obviously relies on the accuracy of this procedure. For this reason, the preamble and detection algorithm must be jointly designed to simultaneously ensure the low-latency and high-reliability constraints.[3] Here, we assume perfect detection to show the upper bound performance of the proposed multiplexing scheme.

B. Computing the eMBB-Oriented RIS Configuration

To assist the eMBB transmission, the eMBB-oriented RIS configuration $\boldsymbol{\Psi}^{\mathrm{e}} \in \mathbb{C}^{N \times N}$ is set to maximize the eMBB SNR. This is attained with coherent passive beamforming, as [19]:

$$\boldsymbol{\Psi}^{\mathrm{e}} = \mathrm{diag}([e^{-j\theta_1^{\mathrm{e}}} \ \cdots \ e^{-j\theta_N^{\mathrm{e}}}]^{\mathsf{T}}), \ \text{where} \qquad (9)$$
$$\theta_n^{\mathrm{e}} = \arg(g_n) + \arg(h_{\mathrm{e},n}), \ n \in \{1, \ldots, N\}.$$

In such a case, from (4) and (5), the effective channel of the eMBB UE can be simplified to

$$\mathbf{g}\boldsymbol{\Psi}^{\mathrm{e}}\mathbf{h}_{\mathrm{e}} = \sum_{n=1}^N |g_n||h_{\mathrm{e},n}| = N\sqrt{\gamma(\mathbf{q}_{\mathrm{BS}}, \mathbf{q}_{\mathrm{RIS}})\gamma(\mathbf{q}_{\mathrm{e}}, \mathbf{q}_{\mathrm{RIS}})}. \quad (10)$$

Therefore, the RIS provides high SE for the eMBB UE by yielding the maximum array gain of N^2 for its channel.

C. Computing the URLLC-Oriented RIS Configurations

At the BS, the computation of a RIS configuration to assist the URLLC transmission is challenging, since only eMBB CSI is available at the BS. The idea is to find a configuration that mitigates the interference caused by the eMBB traffic to the URLLC one. To that end, we present two methods for computing the URLLC-oriented configuration. The first one is a heuristic based on *phasors rotation*. The second one is an *alternating projection* algorithm to approximate a configuration that nulls the eMBB interference. Both strategies use only the BS' CSI of the eMBB UE. Intuitively, the first method tries to cancel out the channel gain of the eMBB UE by compensating the phase shifts of the RIS elements via subtraction, while the second achieves it by relying on a conventional optimization method. Motivated to show the upper bound performance of the proposed scheme, we assume perfect CSI, leaving the study of the impact of imperfect CSI for future work.

Method 1: *Phasors rotation (PR)*. Let us define the problem of finding a RIS configuration that minimizes the equivalent

---

[2] In practice, this active element could also be the antenna of the communication interface used to control the RIS [4], making it a viable solution.

[3] For example, focusing on the URLLC service, the robust scheme proposed in [18] introduces a short preamble comprised of a single orthogonal frequency-division multiplexing (OFDM) symbol, which is detected at the receiver using differential detection. Such an algorithm could be easily deployed at a hybrid RIS with low signal processing capacity.

channel gain of the eMBB UE, given that the eMBB CSI is known,

$$\min_{\boldsymbol{\Psi} \in \mathbb{C}^{N \times N}} \quad |\mathbf{g}\boldsymbol{\Psi}\mathbf{h}_{\mathrm{e}}| = \left|\sum_{n=1}^{N} g_n \psi_n h_{\mathrm{e},n}\right|, \tag{11a}$$

$$\text{subject to} \quad |\psi_n| = 1, \ \forall n \in \{1, \dots, N\}. \tag{11b}$$

This problem is not convex due to the unit modulus constraints of the reflection coefficients. However, notice that the equivalent channel gain is lower-bounded such that $|\mathbf{g}\boldsymbol{\Psi}\mathbf{h}_{\mathrm{e}}| \geq 0$. Therefore, our goal is to find the reflection coefficients that make the equivalent channel gain to equal this lower bound.

We start by presenting a heuristic algorithm with low computational complexity, which yields a sub-optimal solution to problem (11). The heuristic is based on the representation of the eMBB cascaded channels as phasors, and the idea that we can individually rotate them so that they cancel each other out, nulling the eMBB channel; this is made by dividing the RIS elements into two sets, where the goal of one of the sets is to eliminate the contribution of the other. Let the cascaded channel link that passes through the n-th RIS element be represented by the phasor such that

$$A_n e^{j\omega_n} \triangleq g_n \psi_n h_{\mathrm{e},n}, \tag{12}$$

where $A_n = |g_n||h_{\mathrm{e},n}|$ is the phasor's amplitude, and $\omega_n = \arg(g_n) + \arg(h_{\mathrm{e},n}) - \theta_n$ is the phasor's angle. Let us define the sets of RIS elements $\mathcal{N}_0$ and $\mathcal{N}_\pi$ such that $\mathcal{N}_0 \cup \mathcal{N}_\pi = \{1, \dots, N\}$ and $\mathcal{N}_0 \cap \mathcal{N}_\pi = \emptyset$. The RIS elements are configured with the following phase shift according to the set they belong

$$\theta_n^{\mathrm{u}} = \begin{cases} \arg(g_n) + \arg(h_{\mathrm{e},n}), & n \in \mathcal{N}_0 \\ \pi + \arg(g_n) + \arg(h_{\mathrm{e},n}), & n \in \mathcal{N}_\pi \end{cases}. \tag{13}$$

Using the configuration $\boldsymbol{\Psi}^{\mathrm{u}} = \mathrm{diag}([e^{-j\theta_1^{\mathrm{u}}} \ \cdots \ e^{-j\theta_N^{\mathrm{u}}}]^{\mathsf{T}})$, the cascaded channels belonging to sets $\mathcal{N}_0$ and $\mathcal{N}_\pi$ are out of phase, since $\omega_n = 0$ if $n \in \mathcal{N}_0$ and $\omega_n = -\pi$ if $n \in \mathcal{N}_\pi$. Therefore, from (12) and (13), the effective channel gain of the eMBB UE with this configuration is equal to

$$|\mathbf{g}\boldsymbol{\Psi}^{\mathrm{u}}\mathbf{h}_{\mathrm{e}}| = \left|\sum_{n=1}^{N} A_n e^{j\omega_n}\right| = \left|\sum_{n \in \mathcal{N}_0} A_n - \sum_{n' \in \mathcal{N}_\pi} A_{n'}\right|. \tag{14}$$

Thus, to mitigate the interference caused by the eMBB traffic, we need to determine the sets $\mathcal{N}_0$ and $\mathcal{N}_\pi$ that approximately null (14). Since each cascaded channel can belong to either $\mathcal{N}_0$ or $\mathcal{N}_\pi$, minimizing (14) is a combinatorial optimization problem with 2^N candidate solutions. As this is not tractable even for moderate size RISs, in Algorithm 1 we present an intuitive method for determining $\mathcal{N}_0$ and $\mathcal{N}_\pi$, approximating a solution that minimizes (14) in feasible computation time.

The algorithm works as follows. Initially, the amplitudes of the phasors representing the cascaded channels are computed. Then, the algorithm finds an integer number $1 \leq N^* \leq N$ such that the sum of the amplitudes of the N^* shortest phasors is as close as possible to the sum of the amplitudes of the $N - N^*$ remaining ones. Finally, the set $\mathcal{N}_0$ is created with the indices of the elements associated with the N^* shortest phasors, while $\mathcal{N}_\pi$ is created with the indices of the remaining ones. In the algorithm, $\mu(\cdot)$ is the function that maps the indices of $(\alpha_i)_{i=1}^{N}$ to the respective indices of $\{A_n\}_{n=1}^{N}$.

Algorithm 1 Phasors rotation algorithm to approximate a RIS configuration that minimizes (14).

input: The channel vectors $\mathbf{g}$ and $\mathbf{h}_{\mathrm{e}}$
output: The RIS configuration $\boldsymbol{\Psi}^{\mathrm{u}}$
1: $A_n \leftarrow |g_n||h_{\mathrm{e},n}|$
2: $(\alpha_i)_{i=1}^{N} \leftarrow \mathrm{sort}(A_1, \dots, A_N)$
3: $N^* \leftarrow \underset{1 \leq N' \leq N}{\arg\min} \left|\sum_{i=1}^{N'} \alpha_i - \sum_{i'=N'+1}^{N} \alpha_{i'}\right|$
4: $\mathcal{N}_0 \leftarrow \{\mu(1), \dots, \mu(N^*)\}$
5: $\mathcal{N}_\pi \leftarrow \{\mu(N^* + 1), \dots, \mu(N)\}$
6: $\theta_n^{\mathrm{u}} \leftarrow \begin{cases} \arg(g_n) + \arg(h_{\mathrm{e},n}), & n \in \mathcal{N}_0 \\ \pi + \arg(g_n) + \arg(h_{\mathrm{e},n}), & n \in \mathcal{N}_\pi \end{cases}, \forall n$
7: $\boldsymbol{\Psi}^{\mathrm{u}} \leftarrow \mathrm{diag}([e^{-\theta_1^{\mathrm{u}}} \ \cdots \ e^{-\theta_N^{\mathrm{u}}}])$
8: **return** $\boldsymbol{\Psi}^{\mathrm{u}}$

Method 2: *Interference Nulling (IN)*. The second method for optimizing a configuration to assist the URLLC traffic is based on IN, an approach employed commonly to mitigate interference in different multi-user setups. Let $\boldsymbol{\psi} \in \mathbb{C}^N$ such that $\boldsymbol{\psi} = \mathrm{diag}(\boldsymbol{\Psi})$ denotes the vector with the RIS reflection coefficients. Then, the effective channel of the eMBB UE can be rewritten as $\mathbf{g}\boldsymbol{\Psi}\mathbf{h}_{\mathrm{e}} = \mathbf{g}\,\mathrm{diag}(\mathbf{h}_{\mathrm{e}})\,\boldsymbol{\psi}$. Based on this representation of the effective channel, the problem of finding a RIS configuration that nulls the eMBB interference at the BS can be cast as the optimization problem

$$\text{find} \quad \boldsymbol{\psi} \in \mathbb{C}^N, \tag{15a}$$

$$\text{subject to} \quad \mathbf{g}\,\mathrm{diag}(\mathbf{h}_{\mathrm{e}})\,\boldsymbol{\psi} = 0, \tag{15b}$$

$$|\psi_n| = 1, \ \forall n \in \{1, \dots, N\}, \tag{15c}$$

where (15b) ensures that the eMBB traffic does not interfere at the BS. Similarly to (11), this problem is not convex due to the unit modulus constraints (15c). However, [17] proposed an alternate projection algorithm that approximates a solution to this problem with a high probability of convergence.

In this sense, Algorithm 2 presents an adaption of the alternating projection algorithm in [17] that iteratively approximates a solution to problem (15). During each iteration $t \in \mathbb{Z}_+$, the vector of reflection coefficients $\boldsymbol{\psi}_{t-1}$ is projected sequentially onto the set $\{\boldsymbol{\psi} \in \mathbb{C}^N \mid \mathbf{g}\,\mathrm{diag}(\mathbf{h}_{\mathrm{e}})\,\boldsymbol{\psi} = 0\}$, then onto the set $\{\boldsymbol{\psi} \in \mathbb{C}^N \mid |\psi_n| = 1, \forall n \in \{1, \dots, N\}\}$. The projection operators consider the smallest Euclidean distance from $\boldsymbol{\psi}_{t-1}$ to a point in the projected set, derived according to [17, eq. (20)]. The iterations are interrupted when a stop criterion is satisfied. We used early stopping and maximum iterations as stopping criteria.

IV. ANALYSIS

In this section, we introduce the metrics used in performance analysis of the proposed multiplexing scheme.

A. Performance Analysis

By using the RIS configurations in Sections III-B and III-C, we present expressions for the outage probabilities achieved by the coexistent eMBB and URLLC UEs. Initially, considering the RIS configuration $\boldsymbol{\Psi}^{\mathrm{e}}$ in (9), the instantaneous mutual

Algorithm 2 Alternating projection algorithm for IN, approximating a RIS configuration that solves (15).

---

input: The channel vectors $\mathbf{g}$ and $\mathbf{h}_e$, and the initial RIS reflection coefficients $\boldsymbol{\psi}_0$

output: The RIS configuration $\boldsymbol{\Psi}^u$

1: $\mathbf{v} \leftarrow \frac{\mathbf{g}\,\mathrm{diag}(\mathbf{h}_e)}{\|\mathbf{g}\,\mathrm{diag}(\mathbf{h}_e)\|_2}$

2: $t \leftarrow 1$

3: **repeat**

4: $\quad \tilde{\boldsymbol{\psi}} \leftarrow \boldsymbol{\psi}_{t-1} - (\mathbf{v}\boldsymbol{\psi}_{t-1})\mathbf{v}^H$

5: $\quad \boldsymbol{\psi}_t \leftarrow \left[\frac{\tilde{\psi}_1}{|\tilde{\psi}_1|} \cdots \frac{\tilde{\psi}_N}{|\tilde{\psi}_N|} \right]^\mathsf{T}$

6: $\quad t \leftarrow t + 1$

7: **until** stopping criterion is satisfied

8: $\boldsymbol{\Psi}^u \leftarrow \mathrm{diag}(\boldsymbol{\psi}_{t-1})$

9: **return** $\boldsymbol{\Psi}^u$

---

information per mini-slot of the eMBB data stream at the BS can be derived as

$$I_e(p_e) \triangleq \frac{1}{M} \sum_{m=1}^{M} (1 - \xi) \log_2(1 + \Gamma_{e,m}(\boldsymbol{\Psi}^e)),$$

$$= (1 - \xi) \log_2 \left(1 + \frac{p_e(\sum_{n=1}^{N} |g_n||h_{e,n}|)^2}{\sigma^2} \right), \quad (16)$$

where the pre-log term $\xi = (M_p + 2M_s + m)/M$ accounts for the mini-slots when the transmission of the URLLC preamble, payload and RIS configuration switching occurs. Similarly, the instantaneous mutual information per mini-slot of the URLLC data stream considering the RIS configuration $\boldsymbol{\Psi}^u$ computed by Algorithms 1 or 2 is derived as

$$I_u(p_u, p_e) \triangleq \frac{1}{M_u} \sum_{m \in \mathcal{M}_u} \log_2(1 + \Gamma_{u,m}(\boldsymbol{\Psi}^u)),$$

$$= \log_2 \left(1 + \frac{p_u|\mathbf{g}\boldsymbol{\Psi}^u\mathbf{h}_u|^2}{p_e|\mathbf{g}\boldsymbol{\Psi}^u\mathbf{h}_e|^2 + \sigma^2} \right). \quad (17)$$

Therefore, given constant transmit powers, the outage probabilities of the eMBB and URLLC UEs as functions of the SEs per mini-slot, $r_\iota > 0$, are respectively equal to

$$P_e(r_e) \triangleq \Pr\{I_e(p_e) < r_e\} \text{ and } P_u(r_u) \triangleq \Pr\{I_e(p_u, p_e) < r_u\}.$$

B. Latency Analysis

From Fig. 1, one can identify that the latency introduced by the proposed scheme to the URLLC traffic is governed by three parts: **a)** the transmission of the URLLC preamble, **b)** the delay due to processing of the preamble and switching between configurations at the RIS, **c)** and the transmission of the URLLC payload symbols. Neglecting the propagation delay, the latency introduced by the transmission of the URLLC preamble and payload are respectively $M_p T_m$ and $M_u T_m$. Moreover, we let $D_{proc} > 0$ be a constant that accounts for the time needed to process the preamble at the RIS and detect the start of the URLLC traffic, whose value depends on the overall structure of the adopted detection algorithm and its computational complexity. Also, recall that the delay for the RIS to switch to the URLLC-oriented configuration is $M_s T_m$. Then, one can define the URLLC latency as

$$D = M_p T_m + M_u T_m + D_{proc} + M_s T_m. \quad (18)$$

If the processing delay is negligible compared to the mini-slot duration, a reasonable approximation for the URLLC latency is $D \approx (M_p + M_s + M_u)T_m$. Due to space limitations, we chose to focus on latency results in a future work.

V. NUMERICAL RESULTS

Now, we present numerical simulations to discuss the performance of the proposed scheme for multiplexing eMBB and URLLC services. In the simulations, we assume that $\lambda = 0.1$ m, $\beta = 3.67$, $\gamma_0 = 1$, $d_0 = 1$ m, and $\sigma^2 = -90$ dBm. Moreover, we consider $M_p = M_s = 1$ mini-slot and $M_u = 2$ mini-slots. The RIS is a square surface placed at $\mathbf{q}_{RIS} = \mathbf{0}_3$ in the yz-plane, pointing towards the direction of the x-axis. The BS is at $\mathbf{q}_{BS} = [\varrho_f/\sqrt{2} \ \varrho_f/\sqrt{2} \ 0]^\mathsf{T}$, where $\varrho_f = \lambda(\sqrt{M} - 1)^2/2$ is the far-field distance of the RIS. The region occupied by the UEs is a volume defined in spherical coordinates by the set $\{(\varrho, \vartheta, \varphi) \mid \varrho_f \leq \varrho \leq 100 \text{ m}, \vartheta_{min} \leq \vartheta \leq \vartheta_{max}, \frac{3\pi}{2} \leq \varphi \leq 2\pi\}$, where the tuple $(\varrho, \vartheta, \varphi)$ denotes, respectively, the radial distance, the polar, and azimuthal angles. Specifically, the angles $\vartheta_{min}, \vartheta_{max}$ are such that the z-coordinates of the UEs lie within $[-3, 3]$ m. The UEs' positions, drawn for each of the 10^7 realizations, are uniformly distributed over this region. *Benchmarks:* To compare the proposed algorithms for computing the URLLC-oriented configuration, we define the following benchmarks: **a)** *Random:* The phase shifts $\{\theta_n^u\}_{n=1}^N$ are drawn from an uniform distribution over the interval $[0, 2\pi)$. **b)** *Missed URLLC preamble:* eMBB-oriented configuration, representing the case where the RIS fails on detecting the start of the URLLC traffic. **c)** *Maximize URLLC SNR:* Ideally, assuming that URLLC CSI is available at the BS prior to its transmission, $\boldsymbol{\Psi}^u$ is set to perform coherent passive beamforming for the URLLC UE. **d)** *IN with URLLC CSI:* Also considering known URLLC CSI, $\boldsymbol{\Psi}^u$ is optimized with an improved version of Algorithm 2, adding one step where the reflection coefficients are projected onto the set of the coefficients that maximize the URLLC SNR.

Figs. 2a and 2b present the URLLC outage probability as a function of the SE. The performance of the configurations computed by the proposed PR and IN algorithms reveal that it is possible to improve the reliability of the URLLC transmission relying only on eMBB CSI. In fact, in Fig. 2b, the IN configuration improves the outage probability of the random one up to 3 orders of magnitude. Comparing the PR and IN algorithms, IN presents outage probability up to 6 times lower. However, the PR algorithm yields a better trade-off due to its computationally simple implementation.

Fig. 2c depicts the URLLC outage probability for a SE of 0.5 bps/Hz as a function of the number of RIS elements. To make a fair comparison, in this result, we set the distances from the RIS to the BS and to the region occupied by the UEs to 18 m, which is the far-field distance for $N = 400$. Notice that the outage probability improves with a bigger surface. However, it is important to remark that the overhead for estimating the eMBB CSI is proportional to N. Hence, in the proposed scheme, there is a trade-off between improving the URLLC outage probability by making the RIS bigger and
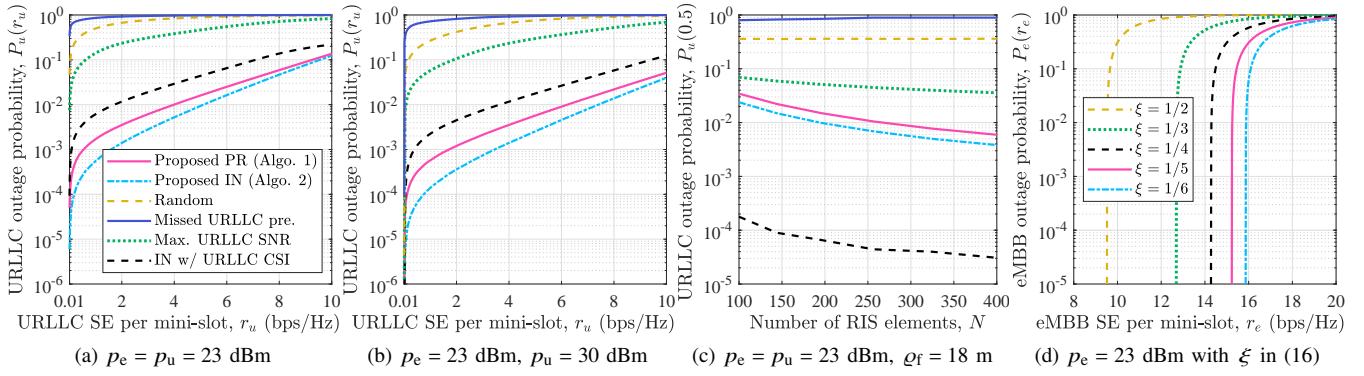
Fig. 2. Outage probabilities of (a, b, c) URLLC UE and (d) eMBB UE. When not otherwise specified, $N = 100$ and $\varrho_{\mathrm{f}} = 4$ m.

the overhead in the training phase. Observe that the benchmark IN with URLLC CSI is better than the proposed approaches in Fig. 2c, which goes against of what has been observed in Figs. 2a and 2b. This happens due to the minimum distance from the RIS to the UEs in Fig. 2c being greater than the one in the others, reducing the eMBB interference and improving the gain from focusing the signal towards the URLLC UE.

Fig. 2d depicts the eMBB outage probability as a function of the SE for different values of the pre-log term ξ in (16) so as to show the impact of increasing overhead. Note that the outage probability improves as ξ decreases, since the proportion of eMBB mini-slots free from URLLC traffic increases. Hence, given the sporadic behavior of the URLLC traffic, high SE can be provided to the eMBB UE by optimizing the number of mini-slots in the payload transmission phase.

VI. CONCLUSIONS

We proposed a RIS-assisted multiplexing scheme to enable the coexistence of UL eMBB and URLLC services. Our scheme relies on the fact the RIS can detect the URLLC preamble locally. Then, based only on the eMBB CSI at the BS, the scheme provides the QoS of both services by computing two RIS configuration at the beginning of each UL frame, one to assist the eMBB UE and the other to assist the URLLC UE. In special, we proposed the phasors rotation and interference nulling algorithms to compute the RIS configuration to assist the URLLC transmission. Comparing the RIS configurations produced by the algorithms with benchmarks, we demonstrated that, when only eMBB CSI is available, the URLLC reliability can be improved with configurations that mitigate the interference generated by the eMBB traffic.

REFERENCES

[1] P. Popovski *et al.*, "5G wireless network slicing for eMBB, URLLC, and mMTC: A communication-theoretic view," *IEEE Access*, vol. 6, pp. 55 765–55 779, Sept. 2018.
[2] M. Z. Chowdhury *et al.*, "6G wireless communication systems: Applications, requirements, technologies, challenges, and research directions," *IEEE Open J. of the Commun. Society*, vol. 1, pp. 957–975, July 2020.
[3] M. Almekhlafi *et al.*, "Enabling URLLC applications through reconfigurable intelligent surfaces: Challenges and potential," *IEEE Internet of Things Mag.*, vol. 5, no. 1, pp. 130–135, Mar. 2022.
[4] M. Di Renzo *et al.*, "Smart radio environments empowered by reconfigurable intelligent surfaces: How it works, state of research, and the road ahead," *IEEE J. on Sel. Areas in Commun.*, vol. 38, no. 11, pp. 2450–2525, July 2020.
[5] H. Xie *et al.*, "User grouping and reflective beamforming for IRS-aided URLLC," *IEEE Wireless Commun. Lett.*, vol. 10, no. 11, pp. 2533–2537, Nov. 2021.
[6] Z. Li *et al.*, "Resource allocation for IRS-assisted uplink URLLC systems," *IEEE Commun. Lett.*, Apr. 2023, early access.
[7] R. Hashemi *et al.*, "Average rate analysis of RIS-aided short packet communication in URLLC systems," in *2021 IEEE Int. Conf. on Commun. Workshops (ICC Workshops)*, 14-24 June 2021, pp. 1–6.
[8] H. Ren *et al.*, "Intelligent reflecting surface-aided URLLC in a factory automation scenario," *IEEE Trans. on Commun.*, vol. 70, no. 1, pp. 707–723, Jan. 2022.
[9] W. R. Ghanem *et al.*, "Joint beamforming and phase shift optimization for multicell IRS-aided OFDMA-URLLC systems," in *2021 IEEE Wireless Commun. and Netw. Conf. (WCNC)*, 29 Mar.-1 Apr. 2021, pp. 1–7.
[10] M. Almekhlafi *et al.*, "Joint resource allocation and phase shift optimization for RIS-aided eMBB/URLLC traffic multiplexing," *IEEE Trans. on Commun.*, vol. 70, no. 2, pp. 1304–1319, Feb. 2022.
[11] H. Zarini *et al.*, "Resource management for multiplexing eMBB and URLLC services over RIS-aided THz communication," *IEEE Trans. on Commun.*, pp. 1–15, Jan. 2023, early access.
[12] W. R. Ghanem *et al.*, "Codebook based two-time scale resource allocation design for IRS-assisted eMBB-URLLC systems," in *2022 IEEE Globecom Workshops (GC Wkshps)*, 4-8 Dec. 2022, pp. 419–425.
[13] V. D. P. Souto *et al.*, "IRS-aided physical layer network slicing for URLLC and eMBB," *IEEE Access*, vol. 9, pp. 163 086–163 098, Dec. 2021.
[14] D. C. Melgarejo *et al.*, "Reconfigurable intelligent surface-aided grant-free access for uplink URLLC," in *2020 2nd 6G Wireless Summit (6G SUMMIT)*, 17-20 Mar. 2020, pp. 1–5.
[15] T. Hou *et al.*, "MIMO-NOMA networks relying on reconfigurable intelligent surface: A signal cancellation-based design," *IEEE Trans. on Commun.*, vol. 68, no. 11, pp. 6932–6944, Nov. 2020.
[16] Z. Ma *et al.*, "Interference suppression for railway wireless communication systems: A reconfigurable intelligent surface approach," *IEEE Trans. on Vehic. Technol.*, vol. 70, no. 11, pp. 11 593–11 603, Nov. 2021.
[17] T. Jiang and W. Yu, "Interference nulling using reconfigurable intelligent surface," *IEEE J. on Sel. Areas in Commun.*, vol. 40, no. 5, pp. 1392–1406, May 2022.
[18] X. Jiang *et al.*, "Packet detection by a single OFDM symbol in URLLC for critical industrial control: A realistic study," *IEEE J. on Sel. Areas in Commun.*, vol. 37, no. 4, pp. 933–946, Apr. 2019.
[19] E. Björnson *et al.*, "Reconfigurable intelligent surfaces: A signal processing perspective with wireless applications," *IEEE Signal Process. Mag.*, vol. 39, no. 2, pp. 135–158, Mar. 2022.